Received: 28 February 2022 | Revised: 14 September 2022 | Accepted: 20 September 2022

DOI: 10.1002/arp.1878

RESEARCH ARTICLE

WILEY

Revisiting Fara: Comparison of merged prospection results of diverse magnetometers with the earliest excavations in ancient Šuruppak from 120 years ago

Sandra E. Hahn[1] | Jörg W. E. Fassbinder[1] | Adelheid Otto[2] | Berthold Einwag[2] | Abbas Ali Al-Hussainy[3]

[1]Department for Earth and Environmental Sciences, Geophysics, Ludwig-Maximilians-Universität, Munich, Germany

[2]Department for Ancient and Modern Cultures, Institute for Near East Archaeology, Ludwig-Maximilians-Universität, Munich, Germany

[3]College of Arts, Deptartment of Archaeology, Al-Qadisiyah University, Al Diwaniyah, Iraq

Correspondence
Sandra E. Hahn, Department for Earth and Environmental Sciences, Geophysics, Ludwig-Maximilians-Universität, Munich, Germany.
Email: sandra.hahn@geophysik.uni-muenchen.de

Funding information
Faculty for Cultural Studies of the LMU; Münchener Universitäts-Gesellschaft

Abstract

Ancient Šuruppak, today Fara, was one of the major Sumerian cities in Mesopotamia. It was situated along one of the ancient watercourses of the Euphrates River. Findings date it back to the Jemdet Nasr period around 3000 BC with a continuous occupation until the end of the Ur III period around 2000 BC. Fara was first explored and excavated by the Deutsche Orient-Gesellschaft in the years 1902 and 1903 under the direction of Walter Andrae. Multiple excavation trenches with lengths up to 900 m transect the 1 km^2 wide mound and are still visible today which enables us to georeference the excavation maps. Today, the 2.2 km^2 wide archaeological area is dry and without any vegetation. Thousands of deep looting pits are covering the majority of mound which not only destroyed its upper metres but also challenge the application of geophysical prospection methods and their interpretation. The magnetometer prospecting of selected areas on and around the mound was carried out with three devices, two total field magnetometers and one gradiometer. The individual survey areas were combined in post-processing by applying a high-pass filter on the total field data sets and multiplying the vertical gradiometer data sets by a factor of two. This approach provides visually uniform magnetograms, despite being obtained by different devices, which simplifies subsequent visual interpretation. These magnetograms enable us to review, and to extend the results of the old excavations. The comparison show a good correlation in accuracy to the old drawings and positive identification of the already excavated features with magnetometry. Highlights of the survey are the discovery of the city wall confirming its existence, the layout of a unique building complex in the centre of the mound, likely a temple, traces of canals inside the city and an evaluation of magnetometer prospection over a looted area.

KEYWORDS

alluvial, archaeo-geophysical interpretation, Fara-Šuruppak, fluxgate gradiometer, looting, magnetic properties, magnetometer prospecting, Mesopotamia, Sumerian city, total field magnetometer

1 | INTRODUCTION

Prima facie, the modern site of Fara, located in the province of al-Qadissiyah in Iraq (see Figure 1), around 40 km south-east from Diwaniyya, appears 'unimpressive' (Heinrich & Andrae, 1931), but it hides the remains of one of the major Sumerian cities of Mesopotamia of the third millennium in plain sight: ancient Šuruppak (Koldewey, 1902b). The pear-shaped tell (see Figure 2) is located in the Mesopotamian alluvial plain at 31.777222 N and 45.510833 E and the main mound's dimension are around 1100 m in length and 600 m in width, and the site covers a total area of 220 ha (Martin, 1988). The tell is generally flat and only rises a few metres above the modern plain with a maximum elevation of 10 m. Fara was situated on the banks one main branches of the Euphrates River, whose course led eventually to Uruk. River avulsions deposited metre-thick layers water-laid silt and sand of varying ages over the last millennia (Morozova, 2005). The havoc of flood events in the Tigris-Euphrates delta finds its climax in the 'Mesopotamian Flood' (Brückner & Engel, 2020), the biblical Deluge, which is mentioned in the Sumerian King List. Šuruppak is named as the seat of the last dynasty 'before the flood'; its King Utnapištim/Ziusudra, biblical Noah, is said to have built the ship to evacuate his people.

The mound of Fara presents itself today as a shallow rise barren of vegetation in the otherwise flat landscape with soils of different shades of brown and red, peppered with plano-convex bricks and pottery sherds, but nowadays disturbed by the myriads of looting holes covering nearly the entire site (Otto et al., 2018; van Ess et al., 2006).

A team of the Deutsche Orient-Gesellschaft started to excavate Fara in June 1902. Robert Koldewey, who also was in charge of the excavation in Babylon, and Walter Andrae shared the direction of the excavation of Fara and the smaller mound of Abu Hatab, both concluding in March 1903. Published letters to the Deutsche Orient-Gesellschaft (Andrae, 1902a, 1902b, 1903; Koldewey, 1902a, 1902b; Nöldeke, 1903) during the time of the excavation are short, focus on the ceramics or other findings and on the adventurous life during excavation. In 1931, Heinrich and Andrae published the excavation results of this campaign (Heinrich & Andrae, 1931) with a more detailed presentation of the findings and brief descriptions of the architectural discoveries. Fifty years later, the results of the German excavations 1902/1903 and the American work in 1931 were analysed by Harriet Martin and brought into the context (Martin, 1988). In combination with her survey results, Martin was able to establish the occupation history throughout the third millennium, with the foundation in the Jemdet Nasr period, an extensive occupation in the Early Dynastic I–IIIa period, and a rapid degression thereafter to almost total abandonment of the site at the end of the Ur III period (Martin, 1983).

FIGURE 1 The region of Mesopotamia is situated within the Tigris-Euphrates river system. It occupies mainly today Iraq. Historical sites are marked red. Modern Iraqi cities are provided for orientation and marked white. Fara is located at one of the branches of the Euphrates River. Satellite data: Google, ©2022 CNES/Airbus, Landsat/Copernicus, Maxar Technologies/U.S. Geological Survey [Colour figure can be viewed at wileyonlinelibrary.com]

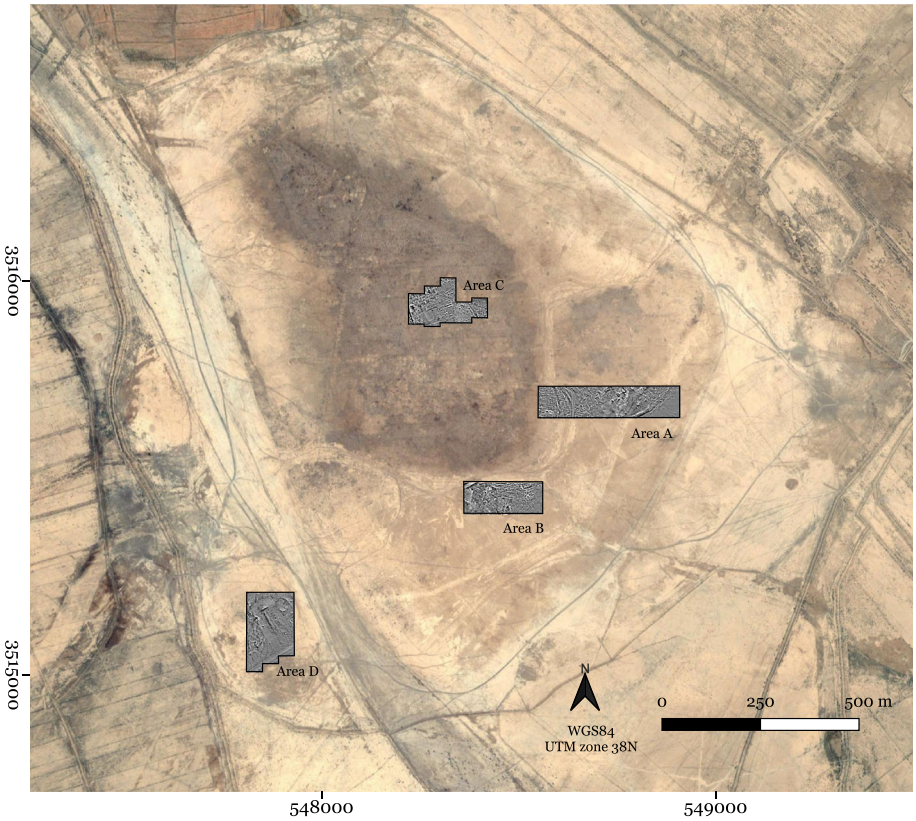

FIGURE 2 Overview on the tell of Fara and its situation. Fara is located today in Iraq, in the province of al-Qadissiyah, around 40 km south-east from Diwaniyya. The main mound is 1 km^2 wide and rises only a few metres from the otherwise flat plan. The archaeolgical area covers around 220 ha and is today without vegetation. Satellite data: Google, ©2022 CNES/Airbus, Landsat/Copernicus, Maxar Technologies / U. S. Geological Survey [Colour figure can be viewed at wileyonlinelibrary.com]

The most advanced method of excavation of the early twenty century was to lay out systematic trenches. In the case of Fara, these were 3 m wide, usually 2 m deep to get through all settlement layers, and up to 900 m long (Koldewey, 1902b). By the end of the campaign, one search trench, heading from north–north-east to south–south-west, and 20 trenches, heading east to west, were transecting the mound (see Figure 3). These excavation trenches, their debris and the Kal'a, the excavation house, are still visible today, especially in the elevation model (Otto & Einwag, 2020). The excavation uncovered dozens of so-called houses of which only around 15 were excavated and later described in detail (Heinrich & Andrae, 1931, pp. 9–17). The walls of the buildings have only five to seven layers of bricks remaining. Baked and mud bricks likely alternate with the designated use of the room or the construction. Further details on the architectural findings have to be re-evaluated with the present knowledge of Sumerian architecture.

The resulting picture of the ancient city of Šuruppak is nevertheless astonishing and does not fit with the supposed structure of a large Early Dynastic city, and with the informations about the city which can be derived through the approximate 1000 cuneiform tablets found in the houses: Is it possible that a city of this importance had no city wall? Where was the palace of the ruler which headed the centralized administration, and where was the temple of the city goddess Sud (Otto & Einwag, 2020, p. 295)? These were the reasons for the magnetometer survey at Fara in 2018, which accompanied the conventional surface survey of the site in the framework of the Fara Regional Survey Project FARSUP (Otto & Einwag, 2020). Magnetometer prospection has proven to be an adequate tool to prospect Mesopotamian sites (e.g., Becker & Fassbinder, 2001; Creekmore, 2010; Darras & Vallet, 2021; Fassbinder et al., 2005; Lambers et al., 2019).

Magnetometer prospection relies on the difference in susceptibility and remanent magnetization between soil and archaeological features (Fassbinder, 2015). The shape of the detected anomalies depend on the shape of the feature, its orientation of the total magnetization (Hahn & Fassbinder, 2021) and the direction of the ambient Earth's magnetic field (Ostner et al., 2019). Instruments commonly used for magnetometer surveys include total field and vertical gradiometers. The former measure the total strength of the superposition of the flux density of buried features and the Earth's magnetic field, while the latter only provide the difference in vertical component between the two probes of this superposition. In the following, we present the results of this magnetometer survey and answer the posed questions: With all the recent looting, what do we still see in the magnetogram and how does this compare to the excavations from 120 years ago? Can magnetometry help to reconstruct the settlement pattern and outline of this major Sumerian city and answer the open questions? Can the data sets of different total field magnetometers and vertical gradiometers from adjoining areas be combined into one visually uniform magnetogram?

2 | METHOD

2.1 | Selection of survey areas

We selected the location of the survey areas mostly upon two factors: how accessible the area was for the magnetometer survey—this

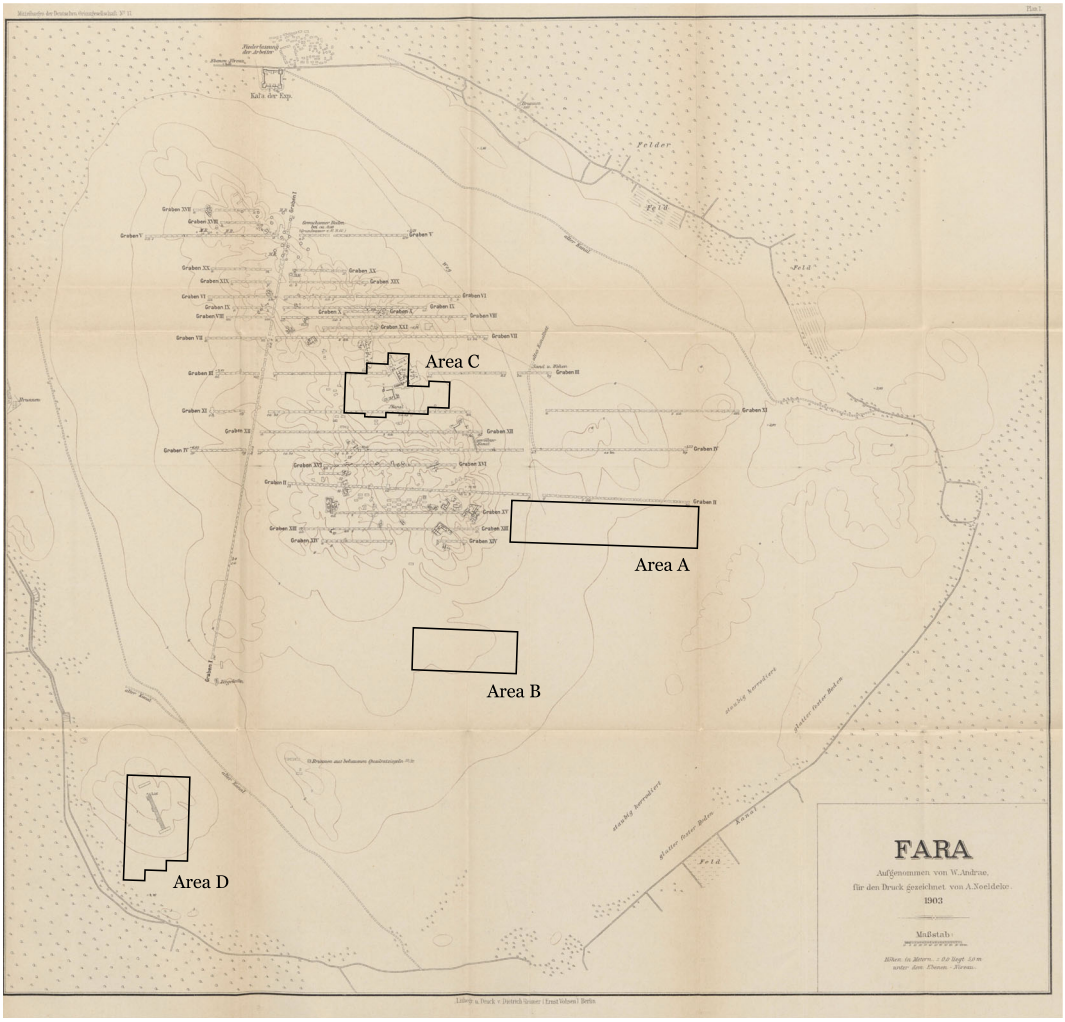

FIGURE 3 1903's overview map of Fara, the excavation trenches and architectural findings, modified after (Heinrich & Andrae, 1931) with the approximate locations of our magnetograms [Colour figure can be viewed at wileyonlinelibrary.com]

depends on the number and size of the looting pits and their debris—and on their location in comparison with Andrae's overview plan (Heinrich & Andrae, 1931, Tafel 1) from 1903 (see Figure 3). The old excavation plan was georeferenced with the help of the still noticeable topography caused by the old excavation trenches. Area A runs parallel and lies south of trench II and lies 55 m east of trench XV, XIII, and XIV. It covers the southern end of a smaller mound east of the main mound. The groundplan of houses had appeared in this area after rainfall and made this a promising area for magnetometry. Area B is situated in the shallow lower town which surrounds the main mound. This area had not been investigated earlier by test trenches, nor had it suffered severe looting due to its flat character (see also Figure 2). Area C is situated in the middle of the main mound, where the central depression separates the southern and the northern half of the site. Andrae's trench III a–c had brought to light a building which differed from other houses in several respects: It was larger and most walls were built from baked bricks; therefore the excavators wondered if this had been a palace or a temple (Heinrich & Andrae, 1931, p. 13). Area D at the separate little mound south-west of the main mound, separated by the ancient river course. Andrae's map shows a wall, which he described as a broad brick wall which terminates at both ends. Andrae wondered if this might have been a part of the fortification wall (Andrae in Heinrich & Andrae, 1931, p. 6).

2.2 | Instruments

For time efficiency, we conducted with three magnetometers the magnetometer survey in Fara in 2018 over a time span of a couple of days: two optical-pumped, self-oscillating Caesium magnetometers in duo-sensor configuration measuring the total field, a Scintrex Smartmag SM4G-special magnetometer and a Geometrics G-858 magnetometer, as well as a vertical vector gradiometer, a Foerster Ferex instrument, with a vertical probe separation of 65 cm indicated by Foerster. Each survey area was separated into three adjacent segments which were scanned by a different magnetometer at the same time. We opted for this procedure mostly due to safety reasons. Since the magnetometer survey team stayed together at one area, they

were more easily guarded by the police man, a requirement of the German university. This also made communication easier, in the event of instrument problems, as the prospectors would not be spread over the tell. The segments of the measurement areas were further divided into individual grids measuring 40 m by 40 m. The resulting data were merged during the data processing. The probes were carried approximately 30 cm above the ground. Because the probe distance of each instrument is 0.5 m, the data resolution is at least 0.1 m by 0.5 m, fulfilling the requirements for archaeological prospection guidelines (Schmidt et al., 2015). Each grid's edge points were georeferenced via GPS measurements.

2.3 | Data processing

The pre-processing of the data focuses on the removal a constant offset caused by the heading error of the caesium probes and interpolating the data to an appointed resolution of 0.25 m by 0.5 m. For each instrument, we combined the measured grids to obtain a graphical data output of their designated survey segments with 'Geoplot' (Geoscan Ltd. UK) software and corrected them for measurement mistakes. The correction for the Geometric's magnetometer is worth mentioning. We were not able to steady the set-up entirely against strong winds during fieldwork, which led to rotation of the probe axis around the rest of the frame. This caused unintentional peaks in our data. We removed these outliners by reducing values three to two times the standard deviation higher than the mean by the mean values. Afterwards, we combined first the Caesium magnetometers' sections. We compensated for the diurnal variation of the Earth's magnetic field by subtracting the calculated mean value of each individual grid from the data values. Further, we adjusted visually the data for linear changes in the Earth's field by multiplying data of single lines with an incrementally increasing or decreasing multiplying factor. For non-linear changes, we added varying values to sections or the whole lines. Eventually, we interpolated the data to a resolution of 0.25 m × 0.25 m. The resulting magnetogram can exemplarily seen for Area A in Figure 4a. To a copy of this data set we apply a high-pass filter to enhance small-scale archaeological feature and suppress the contribution geological sources by removing of larger spatial wavelengths (Aspinall et al., 2009; Scollar, 1969). This effect, along with the correction for the diurnal variation, resembles the idea of gradiometer or pseudo-gradient measurements. Consequently, we were able to combine the high-pass filtered data with the data of the Ferex instrument. Empirically tested, a visual adaptation works best when there is an image high-pass filter with a radius of 10 on the total field data. This visual outcome is presented in Figure 4b. The data of the gradiometer are multiplied by a factor of two for this inclination, around 50° (NCEI Geomagnetic Modeling Team and British Geological Survey, 2019), to compensate for the only one measurement direction of the gradiometer (see Figure 4c). This value is also tested empirically by comparing the standard deviation of both data sets as well as the intensity of similar features. For the interpretation, we studied the combination of total field and gradiometer data as well as the high-pass filtered data and the gradiometer data. For displaying our results, we show only the latter. Additionally for the interpretation, we used drone images of the area and Andrae's drawings (Heinrich & Andrae, 1931; Koldewey, 1902b).

3 | RESULTS AND INTERPRETATION

3.1 | Area A

Immediately adjoining the main tell to the east, we prospected Area A, covering an area of 360 m by 80 m. The resulting magnetogram is shown in Figure 5. In the eastern part of the magnetogram, a prominent feature is noticeable, which we interpret as the city wall. It is traceable over a length of 140 m in the magnetogram, oriented south-west to north-east and has a slightly convex curved shape. The width of the city wall's anomaly ranges between around 6 m to 11 m. The city wall seems separated in different sections by transversal interruption in the feature, forming a pattern comparable to either a 'Kastenmauer' or a casemate. If the compartments were originally filled or not cannot be deduced from the anomaly in the magnetogram. Transversal subdivisions can be found every 6 to 7 m, differently pronounced in the magnetogram, implying a square compartment size of 6–11 m by 6–7 m. The thickness of internal and external wall is likely similar, but the anomaly seems wider at the external wall. Based on the anomaly of the internal wall, a thickness of around 1.5 m can be assumed. The intramural space cannot be clearly determined but can be roughly given with around 3 to 8 m. Overall, the city wall in the southern part of the magnetograms seems to be better preserved because more details a noticeable than in the north-eastern part. The southern part is also more pronounced, but this can be also related to the more east–west orientation of the wall where the direction of Earth's magnetic field enhances the structures. There is no sign of a city gate in the prospected part of the city wall. South-east the city wall, no houses, buildings and streets are detectable. There are some indications for a spacial large-scale feature in the south-eastern part, but the survey did not cover enough of it for an educated guess whether this is of architectural or geological origin. However, the lack of detected archaeological traces indicates that the magnetogram covers an eastern outer part of the ancient city. The features parallel to the city wall can be earth fills, a ditch or parts of the collapsed city wall.

The middle southern part of the magnetogram covering a half elliptic area of 40 m by 120 m seems 'blurry', in the sense that features which are continuing in western, northern and eastern direction are clearer traceable outside this part than inside. The magnetic intensity of the features reduces drastically, so that we are in the instrumental noise of the Foerster Ferex magnetometer. Additionally, the anomalies appear to be broader in this part than in other parts of the magnetogram. Most features' shapes are vague, only strong magnetic features e.g. streets are clearly noticeable. Because this effect does continue over different grids prospected by different instruments, it must be an effect caused by the local soil conditions.

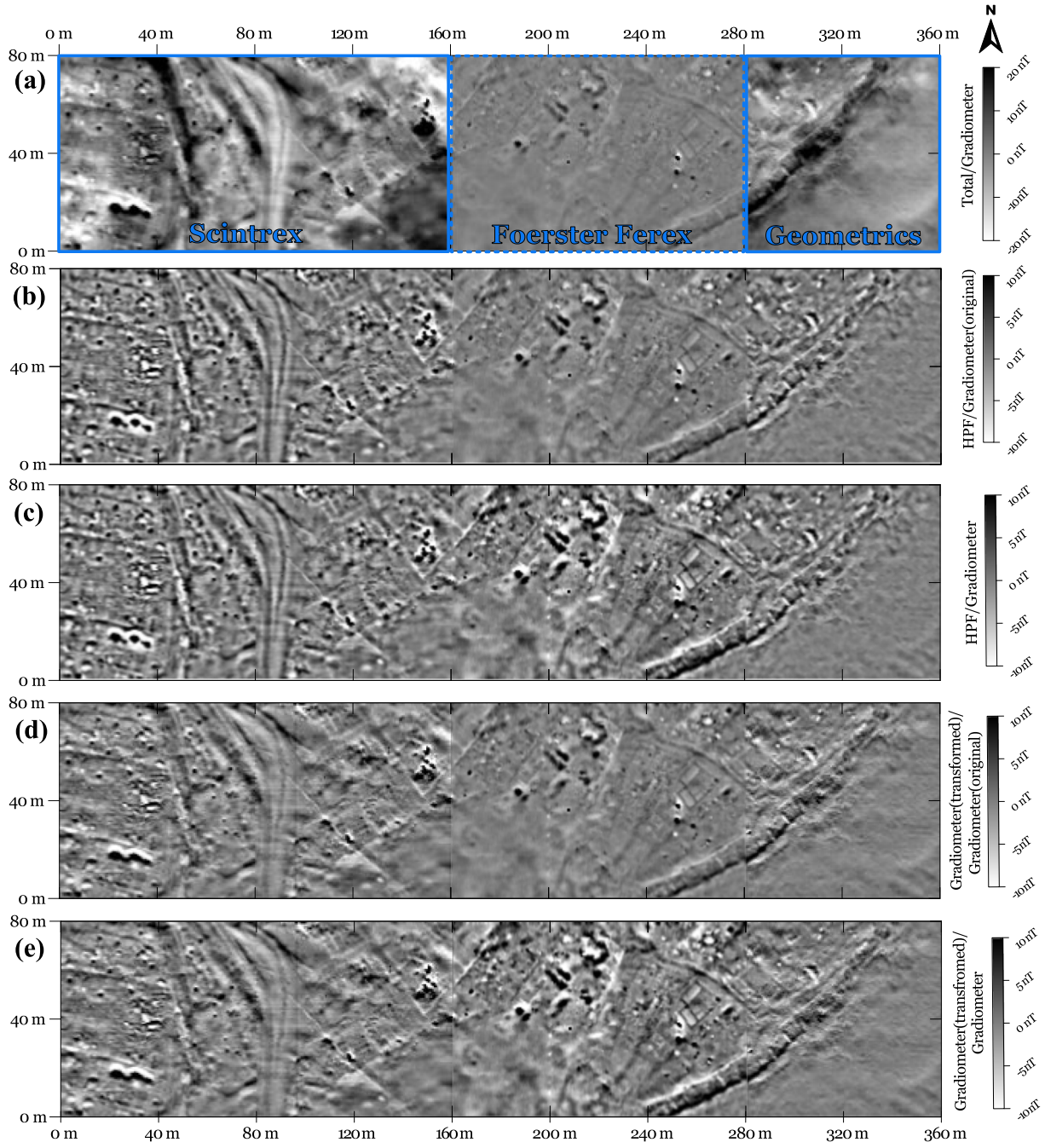

FIGURE 4 (a) Combination of the total field data sets and the vertical gradiometer data sets. (b) Combination of the high-pass filtered total field data sets and the gradiometer data sets. (c) Combination of the high-pass filtered total field data sets and the gradiometer data sets multiplied by 2. (d) Combination of vertical upwards continuation (0.65 m) of the total field data set minus the original data set (transformed gradiometer data) and gradiometer data sets from the Ferex vertical gradiometer. (e) Combination of vertical upwards continuation (0.65 m) of the total field data set minus the original data set (transformed gradiometer data) and gradiometer data sets from the Ferex vertical gradiometer multiplied by 2. [Colour figure can be viewed at wileyonlinelibrary.com]

Most streets are clearly detectable in the magnetogram, with a negative–positive signal sequence. This suggests that their base is supported by material with higher magnetic magnetization, for example, pottery sherds or they follow brick-built vaulted drains. Similar to the city wall, the streets show a north-east–south-west orientation or they are perpendicular to this direction. Majority of the magnetogram shows mostly rectangular building structures of different sizes. The anomalies of the building structures have different magnetic intensities, likely to slight differences in the building material which causes differences in the magnetic properties. The usage of baked bricks can explain the high intensity of some wall's anomalies. We refrain from marking the building structures in detail, because the different

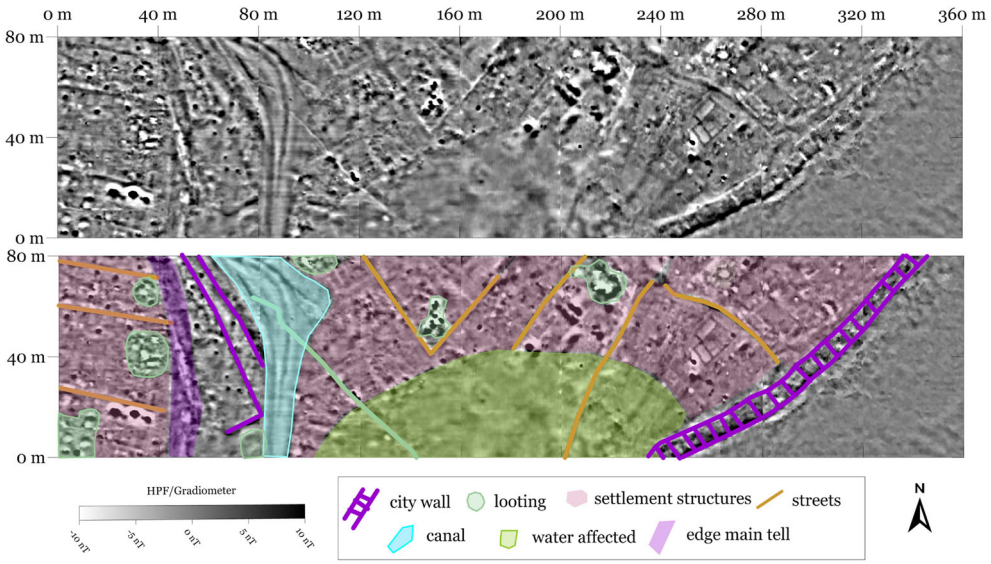

FIGURE 5 Magnetogram of Area A [Colour figure can be viewed at wileyonlinelibrary.com]

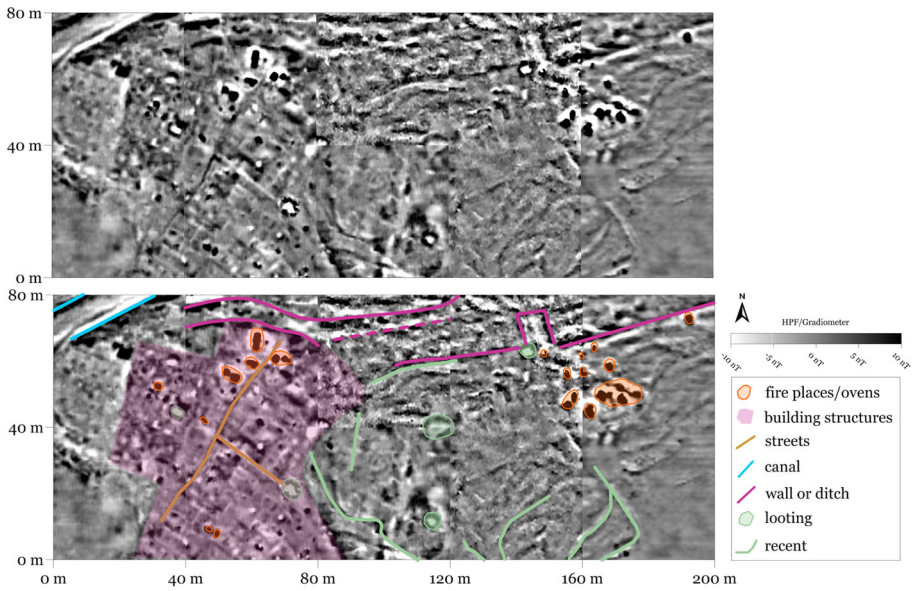

FIGURE 6 Magnetogram of Area B [Colour figure can be viewed at wileyonlinelibrary.com]

anomalies' strength may hide walls and door holes. Also Early Dynastic buildings are built closely together which complicates the assessment of rooms, space between the house and courtyards.

At 80 m, a palaeo-channel or canal is detectable with a north–south orientation with a slightly bent towards the east. Its different accompanying anomalies are suggesting that this waterway changed its course—its deflection towards east—over time. In the east, it seems that it cuts into pre-existing building structures. Therefore, these buildings date before this very eastern course of the canal.

Slightly more westerly, some long linear structures are noticeable. This could be an inner city wall, or perhaps an earlier city wall before the east mound was added to the city. At 40 m, there is a large spacial anomaly recognizable over the whole width of the magnetogram, especially in the total field data. This could be the topographical transition to the main tell. West to this feature, building structures continue on the main tell. Here, streets and houses show a more east–east–south orientation distinguishing them from the lower city. Furthermore, the features on the main tell are not as well pronounced as on the once at lower city. One reason could be the rougher surface on the main tell, caused by looting holes or stronger erosion of the structures.

3.2 | Area B

Directly south-south-east to the main tell we prospected Area B (see Figure 6), covering an area of 200 m by 80 m. The remains of a canal with a north-east orientation are visible in the very upper left corner of the magnetogram. From the digital orthophotos, it is clear that this is the continuation of the canal which is also observable in Area A.

The majority of the western half of the magnetogram shows building structures covering an area of 60 m × 60 m. Again, we refrain

from marking these in detail (see Section 3.1). North-east orientated streets are dividing the building assemblies. Very strong, round or oval anomalies are fireplaces or ovens, some of which are already visible on the surface. We only marked those with an intensity of 30 nT or higher in the merged magnetogram. This is equivalent to 15 nT in the Ferex gradiometer data set and approximately 30 nT in the total field data set. Outside of this area, a set of ovens or fireplaces are recognizable (Figure 6 at 160 and 60 m). East of the marked building structures, there are no clear traces of further houses or buildings. Only some curved features are noticeable. In comparison with the orthophotos, we identify some of these features as erosion channels or runnels, which are exemplarily marked in the magnetogram. Similar looking anomalies could be explained by former courses of erosion channels. Another explanation for these curved feature is the quarrying of mud for pottery or brick production. The possibility of this surmise is supported the set of fireplaces in and outside of building areal and the closeness to the canal.

Two parallel features with a separation of 6 m, possibly wall structures, oriented east–west and traceable over 80 m in the north of the magnetogram. In the middle part of the magnetogram, these two lines are accompanied by another wall structure, around 8.5 m further south with one setback. These walls could belong to a thicker wall, perhaps the inner city wall. It is difficult to deduce more from the magnetogram because this part of the magnetogram seems highly noisy.

3.3 | Area C

Area C (see Figure 7) covers an arbitrary shaped area of around 16 000 m^2 on the main tell. The extent of this area to prospect was limited by looting holes and erosion channels. The multitude of looting holes located at the outer edges of the magnetogram cause strong interferences. The north-eastern corner is still covered by the debris from the 1902 excavation of this building in trench III a–c. The middle part is only 'peppered' by a few looting holes which—if also recognizable in the orthophotos—are marked in the magnetogram. A part of this area was excavated already in 1902 (see Section 4).

A prominent feature is a 27 m × 17 m large rectangle. The area seems magnetically very homogeneous, which indicates that uniform material was used for the whole area as flat smooth basis. At the western corner, a linear feature is prominent, which the magnetogram covers 53 m of its length. The anomaly width is 4 m; the true physical length might be smaller. From the strength of the anomaly, it is reasonable to assume that this is a baked brick construction. However, the anomaly shows semi-regular changes in width. This suggests a road rather than a wall. The variation in intensity also favours the idea of a road as the irregularities could be due to pavement with pottery. Baked brick walls can be seen at different places in the magnetogram. Their lengths vary from 8 to 18 m. Other wall structures noticeable in the magnetogram show a lesser strength in intensity. They are made from a different material, for example, mud bricks or

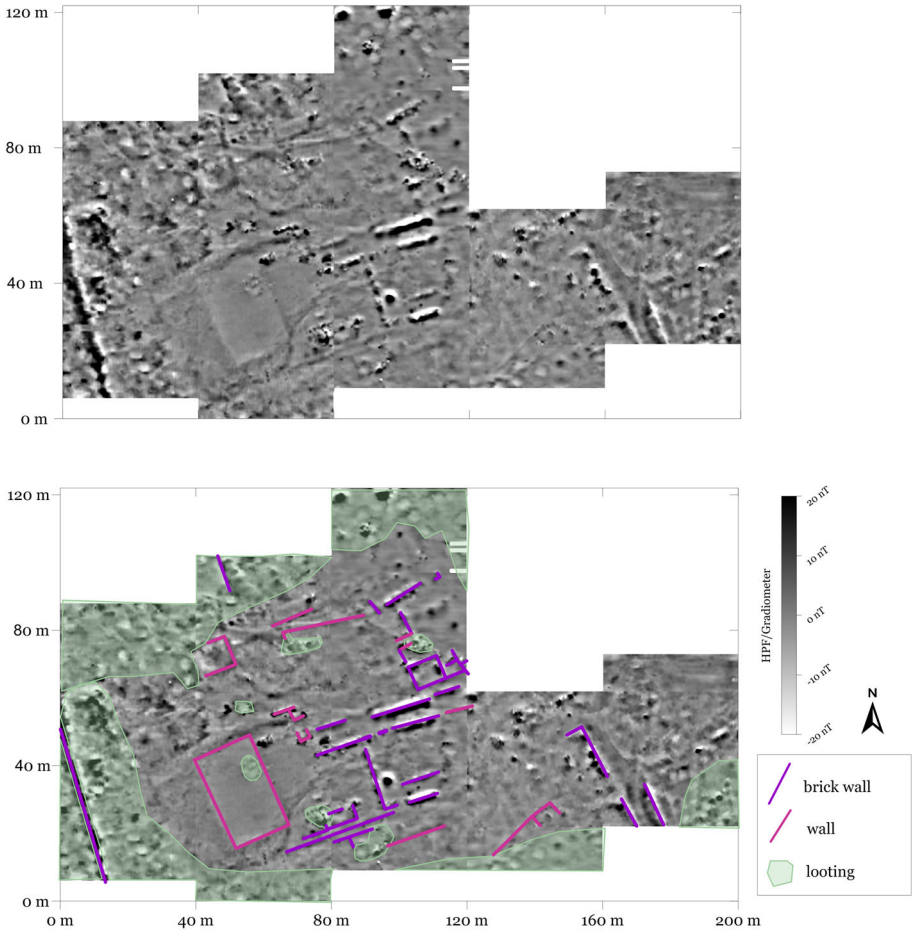

FIGURE 7 Magnetogram of Area C [Colour figure can be viewed at wileyonlinelibrary.com]

slightly fire damaged mud bricks. Almost all of these features, including the baked brick structures, show an east–north-east orientation or perpendicular to this direction. Some features' anomalies are affected by the early 20th century excavation, but mostly, the looting compromises the identification and eventually the interpretation of less distinct features. In other words, if pre-existing archaeological features are not magnetically strong and predominantly linear, their identification over the strong interference caused by the looting holes is difficult.

3.4 | Area D

Approximately 450 m south-west of the main tell, we surveyed Area D (Figure 8) with a size of around 200 m × 120 m. It was situated west of the main watercourse. Large parts of Area D are affected by looting, which we marked in the magnetogram. In this example, the biggest looting pit has a diameter of 28 m. In the unaffected parts, no streets or buildings are detectable. Prominent in the centre of the magnetogram is a strong magnetic anomaly feature which forms a right angle. The high intensity (around +20 nT) implies a construction with a material with a high total magnetization, quite likely baked bricks. Based on the shape of the feature and the surrounding anomalies, we propose that this is the quay wall of one of the city's harbours. The hook-shaped area around the quay wall seems more magnetically homogeneous than other parts of the magnetogram and can be interpret as the basin surrounding the quay. The basin shows a width of 20 to 26 m.

In the south, a parallel running linear features imply an adjacent channel, oriented north-east/south-west, with a width of around 8 m. A continuous linear anomaly along the harbour basis could imply that this channel was still active or at least water-bearing when the harbour was no longer supplied with water. There are some parallel features south the channel, but if these are belonging to another fortification of the channel or a separated construction is unclear because of the lack of survey in this part.

The long side of the quay adjoins orthogonally the channel. From this edge to the northern edge, the quay measures a total length of 110 m. The northern part of the quay shows anomalies with higher intensity; likely a baked brick construction. For the long side, a length of 71 m of this high intensity anomaly can be confirmed. The north edge shows a similar strong anomaly of 21 m in length. The quay seems to resemble a slight T-shape at its northern end. Unanswered remains the true width of the quay, if the shape is symmetric, as well as if the basin continues in the north-east long side of the quay. Anomalies of looting pits on top of areas in question makes it impossible to reconstruct these details.

The southern part of the quay and the basin wall show a lesser anomaly intensity. Because a change in building material is unlikely, one explanation could be different stages of preservation of the baked brick construction.

4 | DISCUSSION

In what follows, we would like to compare our results of the magnetometer prospection to Walter Andrae's plans and Robert Koldewey's and Ernst Heinrich's notes.

As mentioned above, we refrained from enhancing individual houses for all settlement areas and found by magnetometry (which applies to Area A and Area B). Looting and differences in building

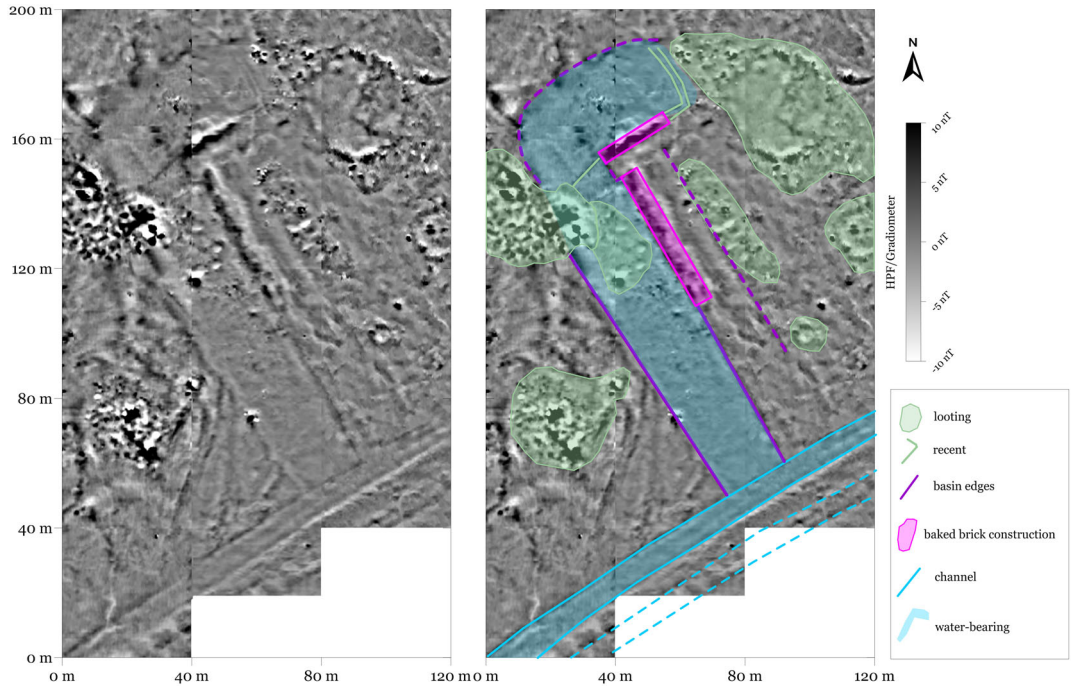

FIGURE 8 Magnetogram of Area D [Colour figure can be viewed at wileyonlinelibrary.com]

material and their magnetization make it hard to correctly identify walls and openings in the walls. Moreover, as Andrae and Heinrich noticed (Heinrich & Andrae, 1931, p. 10), baked bricks, remains of the paving, can be found inside the rooms and the courtyards, which also deludes a clear magnetic response from the walls. What certainly plays a role in the visibility of the wall structures is the usage of baked bricks as wall bases (Andrae, 1903; Heinrich & Andrae, 1931, p. 10). Surprisingly visible are the streets in the settlement areas. Because it is not undoubtedly clear where the recorded vaulted drains were running (Heinrich & Andrae, 1931, p. 10), the magnetometer results are suggesting that they were running below the streets.

Area A lies south, 5 to 10 m distant to trench II (see Section 2.1 and Figure 3). Our identification of buildings or settlement structures visible in the magnetogram are partly confirmed and complemented by drone photos taken after rainfall (Otto & Einwag, 2020). Both the magnetogram and the drone images show streets and the ground plans of houses with several rooms and courtyards. The walls must be close to the surface to be detected with both methods. The drone photos also confirm a continuation of the settlement towards the north (Otto & Einwag, 2020, p. 304, fig. 7). Puzzling therefore is, why there are no descriptions of the architectural structures found in trench II or on this eastern mound in general, or why the excavation trench stopped at this eastern point. With our results, though, we have the answer to Andrae's posed question (Heinrich & Andrae, 1931, p. 7), whether the search trenches extended far enough into the periphery of the tell to trace the city wall! They missed the city wall by a few metres only. In order to trace the course of the city wall, we suggest continuing the magnetometer survey north of area A in future campaigns.

Area B has never been investigated before. Our findings of multiple fireplaces complement the survey results that this area of the lower town was used for pottery production (Otto & Einwag, 2020). In the magnetogram, we see settlement structures. It is unclear if the upper part of the magnetograms shows a continuation of the inner city wall. The visibility of features of this area is clearly more affected by differences in top soil conditions. One explanation for the 'washed out' sections in the magnetograms could be the interaction of the soil and archaeological features with water. Though Fara is relatively dry today, until the 20th century, the mound of Fara was still close to the marshes (Andrae, 1902b; Martin, 1988) and it seems therefore reasonable, that the tell or at least the lower parts of the it were prone to flooding events and/or their soils were saturated with water. Either the "blurry" areas are covered with more alluvial sediments than the other parts or water-logging dissolved partly the iron oxide minerals of the soil and the buried archaeological features. The dissolution of iron oxide minerals decreases the magnetic susceptibility of the soil (Dearing et al., 1995; Hanesch & Scholger, 2005; Thompson & Oldfield, 1986) which also applies to the iron oxides present in the archaeological features which consequently makes them less detectable with magnetometry.

For Area C we compare our results with the details of the building excavated in trench III a–c (Heinrich & Andrae, 1931, pp. 10, 12–13) and its drawing (Heinrich & Andrae, 1931, Tafel 5). The approximate location of the building is provided by Andrae's (3) overview plan, and with the help of the anomalies featured in the magnetogram, we were able to georeference the drawing. For the comparison of the drawing with the relevant part of the magnetogram (Figure 9), we copied the contour of the excavation section and the room numbers given by

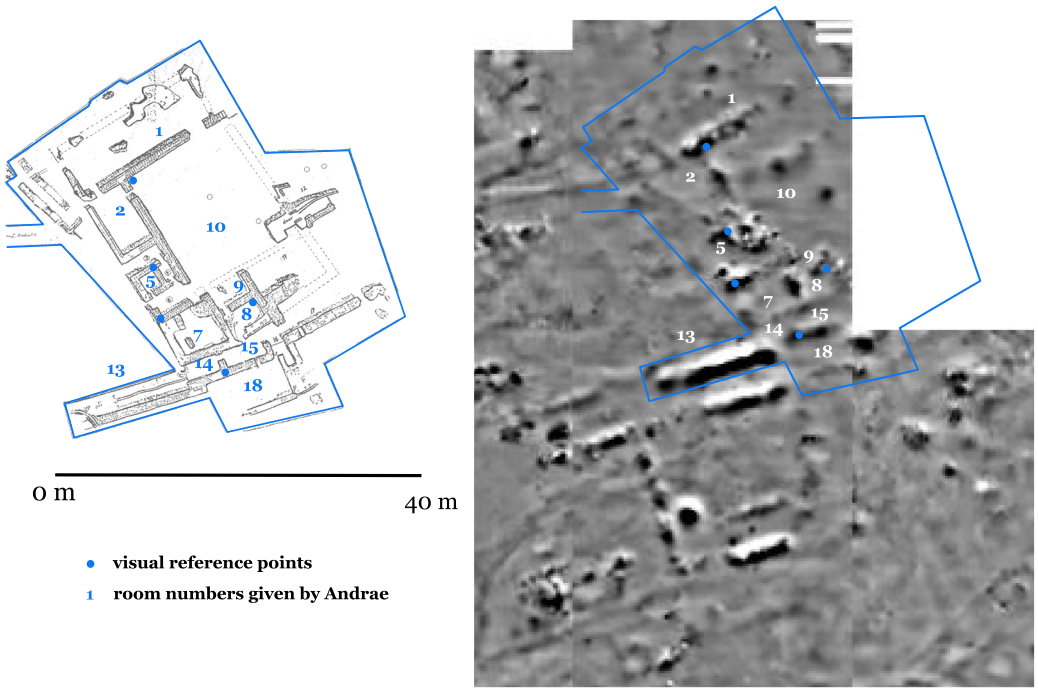

FIGURE 9 Comparision Area C of the map of the building in trench III a–c (Heinrich & Andrae, 1931, Tafel 5) with the magnetometry. The numbers refer to the room numbers given by Andrae and are displayed here in colour and enlarged. The blue dots serve as visual reference points which have the same geographic coordinates. [Colour figure can be viewed at wileyonlinelibrary.com]

Andrae onto the magnetogram. Regrettably, we were only able cover the identical area since the north-eastern part is inaccessible for magnetometer prospecting because of the debris of the 1902 excavation.

Heinrich refers to it as the largest building excavated at Fara (Heinrich & Andrae, 1931, p. 12). Andrae already mentioned the uniqueness of the building, as all its walls were built with baked bricks (Andrae, 1903), thus explaining their good visibility in the magnetogram.

Apparently though, the visibility of features also depends on the state of preservation of the walls. For example, Room 1 (see Figure 9): the southern wall is traceable in the magnetogram in its entire length. The small wall segment in line with this longer wall is also recognizable in the magnetogram. Andrae sketched these two walls in his drawing with throughout with small bricks. This implies a good preservation upon excavation and, based on the magnetogram, a good conservation until today. The western wall of the room was only hinted by Andrae with a few bricks. Its traces are barely visible in the magnetogram. Even more pronounced is the difference in visibility of the walls for Room 2: The eastern and southern walls are identifiable in the magnetogram, again sketched throughout with bricks, while the western wall, sketched with only a few bricks, is magnetically not traceable at all. The more remains are intact, the clearer and more pronounced their anomalies are in the magnetogram. In other words, if there is no change in building material, in case of baked bricks no change in source material and burning process, the strength of the magnetic anomaly of a wall relates dominantly to the amount of bricks preserved of that wall. Similar relationships can be found for all other walls as well. The high correspondence of drawing and magnetogram testimonies Andrae's attention to details and the good conservation of the remains after excavation. It also shows that the width of magnetic anomalies do not reflect necessarily the true physical width. In our example east/west orientated walls show an anomaly width three times higher than the width recorded by Andrae. For the width of magnetic anomalies, the strength of magnetization of the object (high for baked bricks), the burial depth and the physical dimension play a role. The orientation of the object towards the Earth's magnetic field direction also has an impact on the recorded anomaly. In this example, walls orientated east/west are more enhanced than north/south oriented ones. The north-east corner of Room 5 seems to be an exception to this conservation statement. However, the magnetic anomaly caused by the remains of this corner is veiled by the magnetic anomaly caused by the looting at this very spot. Looting disturbs the natural remanent magnetization of the soil that it acquires during pedogenesis or deposition. In the magnetogram, this is usually noticeable as 'freckled' areas with a lot of small dipole anomalies with very small radius. Furthermore, the natural distribution of the magnetic susceptibility is mixed and causes differences in the induced magnetization and consequently in the anomalies. Larger dipole anomalies with higher intensities could be due to iron particles and pieces introduced to the soil during the looting whose strong and spacious anomalies can hide potential archaeological features. Additionally, the edge of the looting holes cause noticeable anomalies, because they vary topographically from the surrounding area. At the edge, more soil and therefore more magnetic material is gathered, explaining the circular character of the anomalies of the looting pits. Comparable features have been recorded by, for example, Fazeli Nashli and Schmidt (2006) or Millaire and Eastaugh (2011).

In the magnetogram, we also see features west of the area covered by Andrae's map of the building in trench III a–c. These anomalies are not distinct enough to provide detailed evidence of further rooms in this part of the magnetogram. The excavation plan for the whole site (Figure 3) shows walls south the building plan whose anomalies we also detect in the magnetogram. The reason why these remains are featured in the overview excavation map but not in the excavation drawing for this building is not evident.

The usage of baked bricks and the larger dimensions of the rooms and the courtyards might imply that the building had a special function. Earlier suggestions were a palace or a temple, while the niches in the southern wall (Andrae, 1903, pp. 9–11) could speak in favour of the latter. Dimensions and layout are comparable to the large Early Dynastic temple at Umm al-Aqarib (Almamori, 2014).

As mentioned above, Andrae's excavation plan shows a uniform feature at the location of Area D. The way it is sketched differs notably from the other features. Andrae was apparently aware of its unique character because he tentatively interpreted this massive built wall, with strong reservations and doubts, as a part of the fortifications (Heinrich & Andrae, 1931, pp. 6–7). We interpret this as a massive construction of baked bricks. The width of the feature is 6.8 m with 6.5 to 7 m long and 2 m strong projections, maybe buttresses, on the south-east side every approximately 22 m (measurements from the georeferenced map). The sketched feature is traceable over a length of 71 m. Directly adjacent towards the south, the map quite likely shows an excavation trench as well as one towards the north, about 15 m from the top of the sketched feature but no features are visible within these trenches. In comparison with our magnetometer results, the sketched feature could be indeed the quay wall constructed from baked brick we detected. The width of the anomaly is at most places around 7 m coinciding with Andrae's map. This implies that the feature lies very close to the surface; otherwise, the deeper burial depth would broaden the detected anomaly. At some places the feature's anomaly is 9 m wide likely resembling the width with the buttresses. The buttresses are not very distinctive in the magnetogram, but there are irregularities and an asymmetry implicating the presence of buttresses. We are able to trace the brick construction for 45 m only, but we are able to detect the basin wall over a length of another 57 m. As already stated, we are not able to say whether the building material changes or not. Andrae's map let us assume it does not. Also with its help, it can be assumed the quay does not continue towards the east. According to our georeferenced map, they just missed the head of the quay by metres.

Some last words on the method we applied on our data to combine the output of total field data sets and the vertical gradiometer data set in one magnetogram. The above mentioned findings highlight the benefit of combing both data sets into one magnetogram. The application of a high-pass filter on the segments of total field data, corrected for diurnal variations, effectively filters out larger spatial wavelengths as theoretically proposed by Scollar (1969). This resembles successfully the visual appearance of the gradiometer data set of

the adjacent segments. By multiplying the data set of the gradiometer by a factor of 2, the lack of signal strength in comparison with the total field data is at least visually compensated. Naturally, the total field data can be divided by the reciprocal of the factor. The lack of signal strength results from measuring only one component of the magnetic flux density. This factor is expected to be mostly dependent on the inclination of Earth's magnetic field in the survey area. Most of the observed anomalies hold a total magnetization parallel or subparallel to the Earth's magnetic field direction. Therefore the ratio of vertical component to absolute strength of an anomaly decreases with decreasing inclination. Consequently, the multiplication factor will be higher for lower inclinations. How the inclination affects the required settings of the image high-pass filter is yet unknown.

To compare our method with a more established method of combining total field and gradiometer data, we transformed the total field data into gradiometer data, as it has been done similar way by e.g. Linford et al. (2007). To do this, we used the programme MagPick (Geometrics) to obtain the upward continuation (e.g., Blakely, 1996) of the entire field data set up to a height of 0.65 m and subtracted these values from the original data set. The result can be seen in Figure 4d. To calculate the pseudo-gradient, one would divide these values by the sensor separation, or in this case more accurately, the vertical height difference between original data set and upward continuation. We deliberately refrain from doing this for a better comparison with the gradiometer data from the Ferex instrument. For further comparison, we also show the Ferex gradiometer data multiplied by 2 in Figure 4e. The high-pass filtered and the transformed gradiometer data of the total field data show good visual agreement (see Figure 4c,d). The transformed gradiometer output still shows a certain 'depth impression' like the total field output which is completely absent in the high-pass filtered output. At least in this example, visually, the latter resembles more closely the Ferex gradiometer output. A comparison of the Figure 4d,e shows that the gradiometer data of the Ferex instruments should also be multiplied by the factor of 2 because of the above mentioned reasons.

For the survey at Fara, the introduced method successfully provides a magnetogram which appears uniform regardless of the instruments used. Visually interpretation of our magnetograms was made significantly simpler because features were easier to trace and compare over the different segments. In our case, the use of a high-pass filter is more favourable, because all visual data processing is then carried out by one software and is therefore more convenient and time-saving.

5 | CONCLUSION

The case study in Fara shows, that magnetometer prospection can offer new insights into already partly excavated sites. The magnetometer survey was conducted with one vertical vector gradiometer and two total field magnetometers on adjoining segments of the measurement areas. The method of applying an image high-pass filter ($R = 10$) on the total field data sets and multiplying the gradiometer data sets by a factor of two successfully provided a combined magnetogram of all three segments in which the change in instrument is imperceptible. The comparison to the old excavation reports and maps shows good correlation with our magnetometry results, especially regarding intact baked brick walls and vice versa, the results of the magnetometer survey bear testimony to the accuracy and richness of details of the excavation maps drawn by Walter Andrae. Heavy looting of the tell not only affects the accessibility of the site but also challenges the further interpretation of magnetograms or even renders parts of them interpretable. Looting pits' anomalies provide strong background interference, which makes the identification of weak magnetic features difficult or impossible. If the magnetic contrast is good and the features are linear, they can be detected even despite heavy looting. This is the case for Area C, where we were able to detect an unknown road in trench III. One further detail which can imply that this building is indeed a temple. One of the major findings are traces of the city wall on the east side of the town, which confirms its existence and prove that the search trenches of 1902 to 1903 were not heading far east enough. We see an intact part of the city wall, which seems to be a casemate wall. Former flooding events might play a role in the sharpness of features in the magnetograms by adding sediments or dissolving magnetic minerals. Nevertheless, the continuation of the magnetometer survey at Fara has the potential to add further and more detailed insights into the settlement structure, which will hopefully be complemented by future excavations.

ACKNOWLEDGEMENTS

The funding for the project was provided by the Faculty for Cultural Studies of the LMU, by the Münchener Universitäts-Gesellschaft and through funds attached to the appointment of A. Otto as chair of Near Eastern Archaeology. We thank the graduate students from al-Qadissiyah University who helped us on the field. Special thanks goes to Marion Scheiblecker who, as part of the geophysicist team, helped to conduct the magnetometer prospection. Further thanks go to the reviewers for their constructive evaluation. We are grateful for their insightful comments on the manuscript and for their encouragement to further elaborate our methodology of merging datasets from diverse magnetometers. Open Access funding enabled and organized by Projekt DEAL.

CONFLICT OF INTEREST

The authors declare that they have no known competing financial interests or personal relationships that could have appeared to influence the work reported in this paper.

DATA AVAILABILITY STATEMENT

The data that support the findings of this study are available from the corresponding author upon reasonable request.

ORCID

Sandra E. Hahn https://orcid.org/0000-0002-3579-8871
Jörg W. E. Fassbinder https://orcid.org/0000-0003-4271-1153

REFERENCES

Almamori, H. O. (2014). The early dynastic monumental buildings at Umm al-Aqarib. *Iraq*, *76*, 149–187.

Andrae, W. (1902a). Aus einem Berichte W. Andrae's über seine Exkursion von Fara nach den südbabylonischen Ruinenstätten (Tell Ĭd, Jŏcha und Hamăm). *Mitteilungen der Deutschen Orient-Gesellschaft*, *16*, 16–24.

Andrae, W. (1902b). Die Umgebung von Fara und Abu Hatab (Fara, Bismăja, Abu Hatab, Hĕtime, Dschidr und Jubă'i). *Mitteilungen der Deutschen Orient-Gesellschaft*, *16*, 24–30.

Andrae, W. (1903). Ausgrabungen in Fara und Abu Hatab. Bericht über die Zeit vom 15. August 1902 bis 10. Januar 1903. *Mitteilungen der Deutschen Orient-Gesellschaft*, *17*, 4–35.

Aspinall, A., Gaffney, C., & Schmidt, A. R. (2009). *Magnetometry for archaeologists*, Vol. 2. Rowman Altamira.

Becker, H., & Fassbinder, J. W. E. (2001). Uruk-City of Gilgamesh (Iraq). First tests in 2001 for magnetic prospecting. *Monuments and Sites*, *6*, 93–97.

Blakely, R. J. (1996). *Potential theory in gravity and magnetic applications*. Cambridge University Press.

Brückner, H., & Engel, M. (2020). Noah's Flood—Probing an ancient narrative using geoscience. In Herget, J., & Fontana, A. (Eds.), *Palaeohydrology: Traces, tracks and trails of extreme events*. Springer International Publishing, pp. 135–151.

Creekmore, A. (2010). The structure of Upper Mesopotamian cities: Insight from fluxgate gradiometer survey at Kazane Höyük, southeastern Turkey. *Archaeological Prospection*, *17*(2), 73–88.

Darras, L., & Vallet, R. (2021). Magnetic signatures of urban structures: Case study from Larsa (Iraq, 6th–1st Millennium BC). *Revue d'archéométrie*, *45*, 1.

Dearing, J. A., Lees, J. A., & White, C. (1995). Mineral magnetic properties of acid gleyed soils under oak and Corsican Pine. *Geoderma*, *68*(4), 309–319.

Fassbinder, J. W. E. (2015). Seeing beneath the farmland, steppe and desert soil: Magnetic prospecting and soil magnetism. *Journal of Archaeological Science*, *56*, 85–95.

Fassbinder, J. W. E., Becker, H., & van Ess, M. (2005). Prospections magnétiques à Uruk (Warka): La cité du roi Gilgamesh (Irak). *Les Dossiers d'archéologie (Dijon)*, *308*, 20–25.

Fazeli Nashli, H., & Schmidt, A. (2006). Tepe Ghabristan: Geophysical Survey Report. *The International Journal of Humanities*, *13*(3), 31–50.

Hahn, S., & Fassbinder, J. W. E. (2021). The effect of remanence in magnetometer prospection. *Revue d'archéométrie*, *45*, 1.

Hanesch, M., & Scholger, R. (2005). The influence of soil type on the magnetic susceptibility measured throughout soil profiles. *Geophysical Journal International*, *161*(1), 50–56. https://academic.oup.com/gji/article-pdf/161/1/50/5898440/161-1-50.pdf

Heinrich, E., & Andrae, W. (1931). *Fara, Deutschen Orient-Gesellschaft in Fara und Abu Hatab 1902/03*. Vorderasiatische Abteilung der Staatlichen Museen Berlin.

Koldewey, R. (1902a). Acht Briefe Dr. Koldewey's (teilweise im Auszug) (Babylon, Fara und Abu Hatab). *Mitteilungen der Deutschen Orient-Gesellschaft*, *15*, 6–24.

Koldewey, R. (1902b). Auszug aus fünf Briefen Dr. Koldewey's (Babylon, Fara und Abu Hatab). *Mitteilungen der Deutschen Orient-Gesellschaft*, *16*, 8–15.

Lambers, L., Fassbinder, J. W. E., Campbell, S., & Hauser, S. (2019). Ancient Charax Spasinou (Iraq)–Interpreting a multi-phase city based on magnetometer survey data. In *New Global Perspectives on Archaeological Prospection: 13th International Conference on Archaeological Prospection*, Archaeopress Publishing Ltd, pp. 201.

Linford, N., Linford, P., Martin, L., & Payne, A. (2007). Recent results from the English Heritage caesium magnetometer system in comparison with recent fluxgate gradiometers. *Archaeological Prospection*, *14*(3), 151–166. https://onlinelibrary.wiley.com/doi/abs/10.1002/arp.313

Martin, H. P. (1983). Settlement patterns at Shuruppak. *Iraq*, *45*(1), 24–31.

Martin, H. P. (1988). *Fara: A reconstruction of the ancient Mesopotamian city of Shuruppak*.

Millaire, J.-F., & Eastaugh, E. (2011). Ancient urban morphology in the Virú Valley, Peru: Remote sensing work at the Gallinazo Group (100 B.C.–A.D. 700). *Journal of Field Archaeology*, *36*(4), 289–297.

Morozova, G. S. (2005). A review of Holocene avulsions of the Tigris and Euphrates rivers and possible effects on the evolution of civilizations in lower Mesopotamia. *Geoarchaeology*, *20*(4), 401–423. https://onlinelibrary.wiley.com/doi/pdf/10.1002/gea.20057

NCEI Geomagnetic Modeling Team and British Geological Survey (2019). World Magnetic Model 2020. NOAA National Centers for Environmental Information.

Nöldeke, A. (1903). Die Rückkehr unserer Expedition aus Fara. *Mitteilungen der Deutschen Orient-Gesellschaft*, *17*, 35–44.

Ostner, S. E., Fassbinder, J. W. E., Parsi, M., Gerlach, I., & Japp, S. (2019). Magnetic prospection close to the magnetic equator: Case studies in the Tigray plateau of Aksum and Yeha, Ethiopia. *13th Int. Conf. on Archaeological Prospection*, *13*, 180–183.

Otto, A., & Einwag, B. (2020). The survey at Fara - Šuruppak 2016-2018. In Otto, A., Herles, M., Kaniuth, K., Korn, L., & Heidenreich, A. (Eds.), *Proceedings of the 11th International Congress on the Archaeology of the Ancient Near East*, Vol. 2. Wiesbaden, pp. 293–306. Harrassowitz Verlag.

Otto, A., Einwag, B., Al-Hussainy, A., Jawdat, J. A. H., Fink, C., & Maaß, H. (2018). Destruction and looting of archaeological sites between Fara/Šuruppak and Išān Bahrīyāt/Isin damage assessment during the Fara Regional Survey Project FARSUP. *Sumer*, *64*, 35–48.

Schmidt, A. R., Linford, P., Linford, N., David, A., Gaffney, C. F., Sarris, A., & Fassbinder, J. W. E. (2015). Eac guidelines for the use of geophysics in archaeology: Questions to ask and points to consider. http://hdl.handle.net/10454/8129

Scollar, I. (1969). Some techniques for the evaluation of archaeological magnetometer surveys. *World Archaeology*, *1*(1), 77–89.

Thompson, R., & Oldfield, F. (1986). *Environmental magnetism*. Allen and Unwin.

van Ess, M., Becker, H., Fassbinder, J. W. E., Kiefl, R., Lingenfelder, I., Schreier, G., & Zevenbergen, A. (2006). *Detection of looting activities at archaeological sites in Iraq using Ikonos imagery*. Herbert Wichmann Verlag.

How to cite this article: Hahn, S. E., Fassbinder, J. W. E., Otto, A., Einwag, B., & Al-Hussainy, A. A. (2022). Revisiting Fara: Comparison of merged prospection results of diverse magnetometers with the earliest excavations in ancient Šuruppak from 120 years ago. *Archaeological Prospection*, 1–13. https://doi.org/10.1002/arp.1878